ELSEVIER

Journal of Fluids and Structures 22 (2006) 493–504

JOURNAL OF FLUIDS AND STRUCTURES

www.elsevier.com/locate/jfs

Hydroelastic coupling of beam finite element model with Wagner theory of water impact

A. Korobkin[a,*], R. Guéret[b], Š. Malenica[b]

[a]Lavrentyev Institute of Hydrodynamics, Novosibirsk 630090, Russia
[b]Bureau Veritas-DR, Paris, France

Received 10 September 2004; accepted 8 January 2006
Available online 7 March 2006

Abstract

The purpose of the paper is to demonstrate the feasibility of the direct coupling of the finite element method for the structural part with a Wagner representation of the hydrodynamic loads during the impact of an elastic body onto the water surface. An efficient and very general method is developed and validated in two dimensions. Advantages of the present method are outlined for the elastic wedge impact problem; however, the method is applicable to any elastic body with small deadrise angle entering water vertically at moderate velocity. Strategy for coupling of this method with commercial finite element codes is discussed.

1. Introduction

The unsteady two-dimensional problem of elastic structural impact onto a liquid free surface is considered. Elastic deflection of the structure is described by the Euler beam equation, while the hydrodynamic loads are evaluated within the so-called Wagner approximation (Wagner, 1932). In Wagner theory, the real shape of the elastic structure is considered within the structural analysis but the hydrodynamic loads are evaluated approximately with the help of so called "flat-disc approximation". Moreover, the boundary conditions are linearized and imposed on an initially undisturbed liquid level.

Wagner theory is formally valid during the initial stage of interaction, when the penetration depth of the entering body is much smaller than the horizontal dimension of the body. In the case of a wedge entering liquid this implies that the deadrise angle of the wedge is small. The Wagner approach cannot be applied to the case of moderate and large deadrise angles. However, for a body with larger deadrise angles one may expect that the hydrodynamic loads acting on such a body during its entry are not large and hydroelastic interaction between the body and the liquid is less important than in the case of the entry problem for elastic bodies with small deadrise angles. For a body with larger deadrise angle (say, an elastic wedge with deadrise angle of 30 or 45°) more advanced theories than that developed by Wagner should be used.

As a candidate, the so called generalized Wagner approach developed by Zhao et al. (1996) and Mei et al. (1999) can be mentioned. In this approach the body boundary condition is imposed on the actual position of the entering body, but the free surface boundary conditions are linearized (in the same way as in Wagner theory) and imposed on the splash-up

*Corresponding author.
E-mail address: sime.malenica@bureauveritas.com (Š. Malenica).

0889-9746/$ - see front matter
doi:10.1016/j.jfluidstructs.2006.01.001

height (in contrast to the Wagner approach, where the linearized free-surface boundary conditions are imposed on the undisturbed initial position of the free surface). The generalized Wagner approach is expected to provide more accurate predictions of the hydrodynamic pressures than those from the classical Wagner approach. For rigid bodies a critical review of more advanced approaches, which are based on Wagner theory, was given by Korobkin (2004).

However, we are unaware of any attempt to use the generalized Wagner approach in hydroelastic calculations. This can be attributed to the fact that the generalized Wagner approach was designed for bodies with moderate deadrise angles, where the classical Wagner theory fails. In ship hydrodynamics impact velocities are of the order of several meters per second and hull platings are relatively thick. Here, local hydroelasticity is not usually a problem for ship sections with moderate deadrise angles, but can be a severe problem for ship sections with small deadrise angles, where the classical Wagner theory can be safely used. If the plate thickness is relatively small, as in the analysis by Lu et al. (2000), or the entry velocity is very high, as in sea ballistics, then hydroelasticity is a problem even for bodies with moderate deadrise angle. For these cases, more advanced hydrodynamic models should be used. Problems of sea ballistics and entry problems for extremely flexible bodies are not considered in this paper.

It should be explained why the simplest theory of water impact developed by Wagner is still the main one used in hydroelastic calculations. First, this theory was designed for bodies with small deadrise angles, which are of primary concern from the point of view of hydroelasticity. Second, this theory was widely tested, so its strengths and weaknesses are well known. On the other hand, more advanced theories, including fully nonlinear models of potential flows with free boundaries, generally contain many technical and numerical 'tricks', which are incorporated, sometimes in an implicit way, with the aim of improving stability and performance of a solver. This can mean that sometimes a solution of more complex equations, which require sophisticated numerical schemes, is not necessarily more accurate than a solution of simplified equations, for which numerical calculations are more transparent and, moreover, a part of them can be performed analytically. Probably, the most complex analysis of the elastic wedge entry problem was performed by Lu et al. (2000) for deadrise angles of 30° and 45°. However, the case of moderate deadrise angles is beyond the scope of this paper. Moreover, Lu et al. expressed the view that validation of their method and "extensive comparison with experimental data is needed before the method is used for practical applications". We can also add that comparison of the so-called "more accurate models" with simplified ones would be helpful, to be sure that these models really provide the high level accuracy claimed by their authors.

Despite its relative simplicity, the theory developed by Wagner and based on the "flat-disk" approximation, correctly predicts the stresses in a horizontal elastic plate subject to wave impact [see Faltinsen et al. (1997)], and in a circular elastic shell entering water at constant velocity (Ionina and Korobkin, 1999). In both cases the normal mode method was used within the Wagner theory and the results were compared with the corresponding experimental ones. For elastic circular shells the results obtained within the Wagner theory were also compared with the numerical results by Arai and Miyauchi (1998) obtained from fully nonlinear potential theory with large deformations of the liquid free surface. In terms of stresses, a fairly good agreement was obtained. A possible explanation of good performance of the Wagner approach in hydroelastic problems of water impact was given by Faltinsen (1997), who wrote "The experimental results suggest that the maximum impact pressures cannot be treated deterministically even in deterministic environmental conditions. The theory does not predict these pressures in a quantitative way. The good agreement between theoretical and experimental bending stresses and deflections shows that it is not necessary to quantitatively predict the large pressures."

Even within the Wagner approach the problem under consideration is coupled and nonlinear. The hydrodynamic loads on the structure and the structure deflections have to be determined at the same time, together with the extent of the wetted part of the body. Evolution of the wetted body area in time is an important characteristic of the impact, which strongly affects the magnitude of the loads.

The problem of elastic beam impact has been intensively studied in connection with wetdeck slamming of a catamaran and entry of an elastic wedge into water. In both cases the elastic structure was modelled either as a homogeneous Euler beam or as a combination of homogeneous beams connected to each other (Kvalsvold and Faltinsen, 1995). The normal mode method was used to represent elastic deflection of the homogeneous structure during the impact. The normal mode method allowed us to calculate the hydrodynamic loads in a simple way by reducing the problem to computation of the added mass matrix elements, which are only dependent on the wetted area of the body. Unfortunately, this is the case only for one homogeneous beam. If the beam is not homogeneous or the structure consists of several homogeneous beams, then the loads are not as easy to compute and this part of the calculation becomes very time consuming.

The finite element method is the main tool in structural analysis. In the present paper, we combine this method with the Wagner approach to develop an efficient numerical algorithm for the analysis of the interaction between a complex elastic structure and the liquid during impact. Only the distribution of the velocity potential along the wetted part of the structure is required to compute the structure deflection and the bending stress distribution in the structure. This result is obvious within linear hydroelasticity; however, the problem under consideration is nonlinear because we do not know in advance the extent of the wetted part of the structure. The decoupling of hydrodynamic and structural analysis utilized in this paper is similar to that used in the normal mode method [see Korobkin (1998), where this decoupling was used for the first time]. Kvalsvold and Faltinsen (1995) used another method of decoupling and clearly recorded the difficulties induced by their decoupling. The technique utilized in the present paper can be viewed as a generalization of the technique used in linear hydroelasticity. The generalization recognises that the wetted area is unknown in advance and has to be determined together with the structural deflection. We do not evaluate the hydrodynamic pressures in the present analysis and consequently the calculations of the velocity potential are reduced within the finite element method to evaluation of the added mass matrix. The elements of the added mass matrix were analytically obtained and this makes the calculations of the structural response fast and efficient. Position and dimension of the contact region between the structure and the liquid are determined from the Wagner condition without additional assumptions. This condition is complicated and nonlinear, but it is shown that the Wagner condition is equivalent to a system of two ordinary differential equations for the coordinates of the contact points. Finally, the original coupled problem is reduced to a nonlinear system of ordinary differential equations for the displacements of the beam elements and the coordinates of the contact points. The system is integrated numerically by the fourth-order Runge–Kutta method. The results obtained by using this method are in very good agreement with the exact results derived previously for the problem of homogeneous plate impact onto a liquid free surface.

The advantages of the present method are outlined for the elastic wedge impact problem. However, the analysis is valid for any blunt elastic structure entering water at moderate velocity.

2. Mathematical model

The plane unsteady problem of an elastic wedge penetrating an ideal and incompressible liquid is considered. Surface tension effects are ignored. Initially ($t' = 0$) the wedge touches the horizontal free surface of the liquid at a single point and starts to move down thereafter with a constant velocity V. The initial contact point is taken as the origin of the Cartesian coordinate system $x'Oy'$ (dimensional variables are denoted by a prime). The line $y' = 0$ corresponds to the liquid free surface at $t' = 0$. The side walls of the wedge are modelled by simply supported Euler beams. The beams are of equal length but of variable thickness. Owing to the different elastic properties of the left and the right wedge walls, the flow caused by the wedge impact is asymmetric with respect to the line $x' = 0$. The initial position of the wedge side walls is described by the equation $y' = |x'|\tan\gamma$, $|x'| < L\cos\gamma$, where γ is the deadrise angle of the equivalent rigid wedge and L is the length of the side walls. The normal deflection of the beam is denoted by $w'(s', t')$, where s' is the coordinate along the initially undeformed side walls, $-L < s' < L$, $s' = 0$ corresponds to the wedge tip and $s' = L$ to the end-point of the right-hand side beam and $s' = -L$ to the end-point of the left-hand side beam. The beams are deforming owing to their interaction with the liquid. The position of the deformed plating of the wedge is given in the parametric form

$$x' = s'\cos\gamma - w'(s', t')\,\mathrm{sgn}(s')\sin\gamma, \tag{1}$$

$$y' = |s'|\sin\gamma + w'(s', t')\cos\gamma - Vt' \quad (-L < s' < L). \tag{2}$$

In this analysis we consider only the case of small deadrise angles γ. We shall determine the liquid flow, the pressure distribution in the liquid region, deflection of the wedge, the stress distribution in the wedge platings and the dimension of the wetted part of the entering wedge under the assumption $\gamma \ll 1$.

Nondimensional variables are used below. The beam length L is taken as the length scale and the impact velocity V as the velocity scale of liquid particles. Assuming that the wedge is rigid and the free surface is undeformed during the penetration, we see that the wedge is totally wetted at instant $T = (L/V)\sin\gamma$ and the vertical displacement of the wedge is equal to $L\sin\gamma$ at this time instant. The quantity T is taken as the time scale and the product $L\sin\gamma$ as the displacement scale, the product VL as the scale of the velocity potential and the quantity $\rho V^2/\sin\gamma$ as the hydrodynamic pressure scale, where ρ is the liquid density. Wagner theory can be applied to the entry problem of a wedge with small deadrise angle γ; see Korobkin (2000). We introduce the small parameter $\varepsilon = \sin\gamma$ and consider the coupled problem of elastic wedge interaction with liquid in the case $\varepsilon \ll 1$.

The plane, potential and nonlinear flow generated by the elastic wedge penetration is described in the nondimensional variables by the velocity potential $\varphi(x, y, t)$ which satisfies the following equations:

$$\varphi_{xx} + \varphi_{yy} = 0, \quad p = -\varphi_t - \frac{1}{2}\varepsilon(\nabla\varphi)^2 - \varepsilon^2\frac{gL}{V^2}\eta(x, t) \quad (\text{in } \Omega(t)), \tag{3}$$

$$p = 0, \quad \eta_t + \varepsilon\eta_x\varphi_x = \varphi_y \quad (\text{on } \partial\Omega_F(t)), \tag{4}$$

$$\varphi_y = -1 + w_t + \varepsilon\frac{1+\cos\gamma w_s}{\cos\gamma - \varepsilon^2 w_s}\varphi_x + \varepsilon^2 w_t \frac{(1-\cos\gamma)/\sin^2\gamma + w_s}{\cos\gamma - \varepsilon^2 w_s} \quad (\text{on } \partial\Omega_S(t)), \tag{5}$$

$$\varphi \to 0 \quad (x^2 + y^2 \to \infty), \tag{6}$$

where g is the gravity acceleration, $\Omega(t)$ is the flow domain which varies with time (see Fig. 1), $\partial\Omega_F(t)$ is the free surface of the flow boundary, $\partial\Omega_F(t) = \{x, y | y = \varepsilon\eta(x,t), x < -b(t) \text{ and } x > a(t)\}$, and $\partial\Omega_S(t)$ is the part of the flow boundary, which is in contact with the entering wedge surface. We write $\partial\Omega_S(t) = \{x, y | y = \varepsilon y_b(x,t), -b(t) < x < a(t)\}$, where the function $y_b(x,t)$ is defined in parametrical form by Eqs. (1) and (2) rewritten in nondimensional variables. It should be noted that the definition of the free surface given above does not account for the flow features close to the intersection points, where jetting occurs and the free surface cannot be projected one-to-one onto the horizontal line. The functions $b(t)$ and $a(t)$ are unknown in advance and have to be determined together with the liquid flow and the wedge wall deflections.

With nondimensional variables, Eqs. (1) and (2) take the form

$$x = s - \varepsilon^2[s(1-\cos\gamma)/\sin^2\gamma + w(s,t)\ \text{sgn}(s)], \tag{7}$$

$$y = \varepsilon[|s| + w(s,t) - t] - \varepsilon^2 w(s,t)(1-\cos\gamma)/\sin^2\gamma. \tag{8}$$

The s-coordinates of the contact points along the deformed platings of the wedge, $s_a(t)$ and $s_b(t)$, are defined by the $x(s_a(t), t, \varepsilon) = a(t)$ and $x(s_b(t), t, \varepsilon) = -b(t)$, respectively.

The beam deflection $w(s,t)$, where $-1 < s < 1$ and $t \geqslant 0$, is governed by the equations

$$m(s)\frac{\partial^2 w}{\partial t^2} + \frac{\partial^2}{\partial s^2}\left(EI(s)\frac{\partial^2 w}{\partial s^2}\right) = q(s,t), \tag{9}$$

$$w = w_{ss} = 0 \quad (s = -1, s = 0, s = 1), \tag{10}$$

$$w = w_t = 0 \quad (t = 0), \tag{11}$$

where $m(s) = m'(sL)/(\rho L)$ is the nondimensional mass distribution, E is Young's modulus of elasticity, $EI(s) = EI'(sL)\sin^2\gamma/(\rho V^2 L^3)$ is the nondimensional rigidity of the beam, and $I'(s')$ is the moment of inertia of the beam cross-section. The hydrodynamic load $q(s,t)$ is given as $q(s,t) = p(x(s,t,\varepsilon), y(s,t,\varepsilon), t)$, where $s_b(t) < s < s_a(t)$, and $q(s,t) = 0$, with $s_a(t) < s < 1$ and $-1 < s < s_b(t)$.

The boundary-value problem (3)–(11) is considered under the additional condition that the components $\partial\Omega_F(t)$ and $\partial\Omega_S(t)$ of the liquid boundary match each other at the intersection points, which provides two equations with respect to

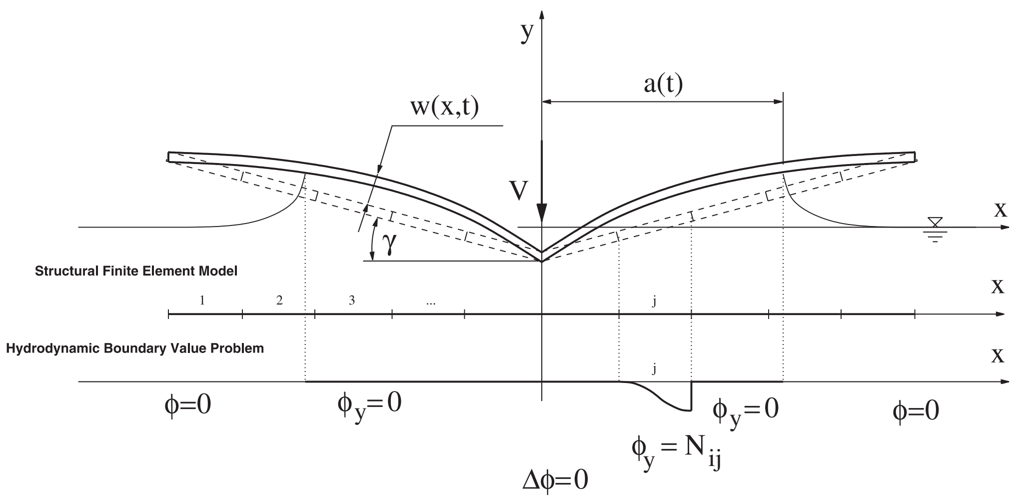

Fig. 1. Basic configuration and definitions.

the functions $a(t)$ and $b(t)$:

$$\eta(a(t), t) = y_b(a(t), t), \quad \eta(-b(t), t) = y_b(-b(t), t). \tag{12}$$

We restrict ourselves to the first-order asymptotics of the solution as $\varepsilon \to 0$. For this case condition (12) was derived by Wagner (1932) and is herein referred to as the Wagner condition. Correspondingly, the boundary-value problem (3)–(12), where $\varepsilon = 0$, is referred to as the Wagner problem for an elastic wedge. More details about the limit $\varepsilon \to 0$ and the Wagner theory for rigid body impact can be found in papers by Howison et al. (1991) and Cointe (1991). Oliver (2002) justified conditions (12). Fraenkel and McLeod (1997) provided rigorous mathematical analysis of the limit $\varepsilon \to 0$ in the problem of rigid wedge entry with small deadrise angle γ.

It is important to notice that within the Wagner formulation the coordinate s along the surface of the structure and the horizontal coordinate x are equal to each other with accuracy of $\mathcal{O}(\varepsilon^2)$ as $\varepsilon \to 0$, the nonlinear term in the Bernoulli equation (3) can be neglected with accuracy of $\mathcal{O}(\varepsilon)$, and the gravity effects can be neglected with the accuracy of $\mathcal{O}(\varepsilon^2)$ once the ratio gL/V^2 is of the order of $\mathcal{O}(1)$ in the Bernoulli equation (3). Moreover, the body boundary condition can be highly simplified with accuracy of $\mathcal{O}(\varepsilon)$ and the kinematic boundary condition (4) can be linearized with accuracy of $\mathcal{O}(\varepsilon)$ and imposed on the initial position of the free surface with the same accuracy. To leading order, the Wagner conditions (12) provide

$$a(t) + w[a(t), t] - t = \eta[a(t), t], \tag{13}$$

$$b(t) + w[-b(t), t] - t = \eta[-b(t), t]. \tag{14}$$

The small influence of gravity effects in water impact problems was discussed by Cointe (1991) and Howison et al. (1991).

Within the Wagner approach adopted here, two-dimensional and potential flow caused by beam impact is described in nondimensional variables by the velocity potential $\varphi(x, y, t)$ which satisfies the following equations:

$$\varphi_{xx} + \varphi_{yy} = 0, \quad p = -\varphi_t \quad (y<0), \tag{15}$$

$$p = 0, \quad \eta_t = \varphi_y \tag{16}$$

$$(y = 0,\ x>a(t) \quad \text{and} \quad x< -b(t)),$$

$$\varphi_y = -1 + w_t \quad (y = 0,\ -b(t)<x<a(t)), \tag{17}$$

$$\varphi \to 0 \quad (x^2 + y^2 \to \infty). \tag{18}$$

The point $(-b(t), 0)$ corresponds to the left edge of the contact region between the entering body and the liquid, and the point $(a(t), 0)$ corresponds to the right edge of this region. The functions $a(t)$ and $b(t)$ are unknown in advance and have to be determined in the solution with the help of Eqs. (13) and (14). In the symmetric case, $b(t) = a(t)$.

The beam deflection $w(x, t)$, where $-1<x<1$ and $t\geqslant 0$, is governed by the equations

$$m(x)\frac{\partial^2 w}{\partial t^2} + \frac{\partial^2}{\partial x^2}\left(EI(x)\frac{\partial^2 w}{\partial x^2}\right) = p(x, 0, t), \tag{19}$$

$$w = w_{xx} = 0 \quad (x = -1, x = 0, x = 1), \tag{20}$$

$$w = w_t = 0 \quad (t = 0), \tag{21}$$

where $p(x, y, t)$ is the hydrodynamic pressure given by the linearized Bernoulli's equation. End conditions (20) represent the simply supported beam and can easily be replaced with more realistic conditions.

The formulated coupled problem (13)–(21) is nonlinear due to Eqs. (13) and (14) with respect to the coordinates of the contact points.

3. Finite element method and coupling

Within the finite element method the beam is divided into N elements and the beam deflection is represented inside each element with the help of four polynomials of the third order $N_{ij}(\xi)$:

$$w(x, t) = \sum_{j=1}^{N}\sum_{i=1}^{4} a_{ji}(t)N_{ij}(\xi), \tag{22}$$

where ξ is the local coordinate within the element j, $-1<\xi<1$, $x=x_j+\ell(\xi+1)/2$, ℓ is the element length, x_1 corresponds to the left edge of the beam and $x_N+\ell$ to the right edge, $x_{j+1}=x_j+\ell$. The unknown coefficients $a_{ji}(t)$ are referred to as principal coordinates of the beam deflection.

The variational form of the Euler beam equation and representation (22) provide a system of $4N$ differential equations with respect to the principal coordinates:

$$\mathbf{M}\ddot{\mathbf{a}}+\mathbf{K}\mathbf{a}=\mathbf{f}(t),$$

$$\mathbf{a}(t)=(a_{11},a_{12},a_{13},a_{14},a_{21},a_{22},\dots)^{\mathrm{T}},$$

$$\mathbf{f}(t)=(f_{11},f_{12},f_{13},f_{14},f_{21},f_{22},\dots)^{\mathrm{T}}, \quad (23)$$

$$f_{ji}(t)=\int_{x_j}^{x_{j+1}} p(x,0,t)N_{ij}(\xi)\,\mathrm{d}x. \quad (24)$$

Note that $p=0$ outside the contact region, therefore $f_{ji}(t)\equiv 0$ if jth element is not wetted. After some manipulations we obtain

$$f_{ji}(t)=-\frac{\mathrm{d}}{\mathrm{d}t}\left[\frac{\ell}{2}\int_{-1}^{1}\varphi\left(x_j+\frac{\ell}{2}(\xi+1),0,t\right)N_{ij}(\xi)\,\mathrm{d}\xi\right]. \quad (25)$$

The coupling procedure is similar to that applied by Malenica (1998), except that the hydrodynamic coefficients are different. Condition (17) and representation (22) allow us to decompose the potential in the contact region as

$$\varphi(x,0,t)=\varphi_0(x,a,b)+\sum_{j=1}^{N}\sum_{i=1}^{4}\dot{a}_{ji}(t)\varphi_{ij}(x,a,b), \quad (26)$$

where $\varphi_{ij}(x,a,b)=\phi_{ij}(x,0,a,b)$ with $\phi_{ij}(x,y,a,b)$ being the solution of the following boundary-value problem

$$\Delta\phi_{ij}=0 \quad (y<0), \quad (27)$$

$$\phi_{ij}=0 \quad (y=0\ x>a \text{ or } x<-b), \quad (28)$$

$$\frac{\partial\phi_{ij}}{\partial y}=N_{ij}[2(x-x_j)/\ell-1] \quad (y=0,\ x\in(x_j,x_{j+1})\cap(-b,a)), \quad (29)$$

$$\frac{\partial\phi_{ij}}{\partial y}=0 \quad (y=0, x\in(-b,a)\backslash(x_j,x_{j+1})) \quad (30)$$

and $\varphi_0(x,a,b)=\phi_0(x,0,a,b)$ with the function $\phi_0(x,y,a,b)$ being the solution of Eqs. (15)–(18) for the rigid wedge case (i.e. $w(x,t)\equiv 0$).

Substituting (26) into (25) and combining the result with (23), we end up with the matrix equation

$$\frac{\mathrm{d}}{\mathrm{d}t}[(\mathbf{M}+\mathbf{S})\dot{\mathbf{a}}+\mathbf{f}_0]+\mathbf{K}\mathbf{a}=0, \quad (31)$$

where $\mathbf{f}_0=\mathbf{f}_0(a,b)$ is the vector-function with components

$$[\mathbf{f}_0]_{ji}=\frac{\ell}{2}\int_{-1}^{1}\varphi_0\left(x_j+\frac{\ell}{2}(\xi+1),a,b\right)N_{ij}(\xi)\,\mathrm{d}\xi \quad (32)$$

and $\mathbf{S}$ is the matrix of added masses, $\mathbf{S}=\mathbf{S}(a,b)$, with elements

$$[\mathbf{S}]_{ji}^{nm}=\frac{\ell}{2}\int_{-1}^{1}\varphi_{mn}\left(x_j+\frac{\ell}{2}(\xi+1),a,b\right)N_{ij}(\xi)\,\mathrm{d}\xi. \quad (33)$$

It is convenient to introduce a new unknown vector $\mathbf{d}=(\mathbf{M}+\mathbf{S})\dot{\mathbf{a}}+\mathbf{f}_0$, with the help of which the original coupled problem is reduced to the system of ordinary differential equations [see Korobkin (1998) for more details]

$$\dot{\mathbf{d}}=-\mathbf{K}\mathbf{a}, \quad (34)$$

$$\dot{\mathbf{a}}=(\mathbf{M}+\mathbf{S}(a,b))^{-1}[\mathbf{d}-\mathbf{f}_0(a,b)]. \quad (35)$$

The initial conditions are $\mathbf{a}(0)=0, \mathbf{d}(0)=0$.

It is important to note that the Wagner conditions (13) and (14) should also be reformulated according to the finite element representation (22), in order to properly close the problem. The details are given in Section 5.

4. Hydrodynamic coefficients

The main difficulty of the present analysis is the evaluation of the added mass matrix **S**, excitation vector $\mathbf{f}_0$ and the functions $a(t), b(t)$. Here we concentrate on the evaluation of the added mass matrix.

Eq. (33) provides

$$[\mathbf{S}]_{ji}^{nm} = \int_{x_j}^{x_{j+1}} \varphi_{mn}(x,a,b) N_{ij}\left(\frac{2}{\ell}[x-x_j]-1\right)\mathrm{d}x, \tag{36}$$

where $1 \leqslant n, j \leqslant N$, $m, i = 1,2,3,4$. It should be noted once again that in (36) only the numbers j and n, for which both intervals $[x_j, x_{j+1}]$ and $[x_n, x_{n+1}]$ have non-empty intersections with the contact region $[-b, a]$, are considered. For all other numbers j and n the integral in (36) is equal to zero.

It is convenient to introduce the new function

$$\hat{N}_{ij}(x) = \begin{cases} 0, & x > x_{j+1}, x < x_j, \\ N_{ij}[2[x-x_j]/\ell - 1], & x_j < x < x_{j+1}, \end{cases}$$

with the help of which integral (36) takes the form

$$[\mathbf{S}]_{ji}^{nm}(a,b) = \int_{-b}^{a} \varphi_{mn}(x,a,b)\hat{N}_{ij}(x)\,\mathrm{d}x. \tag{37}$$

Denoting $\tilde{N}_{ij}(x) = \int_{-b}^{x} \hat{N}_{ij}(x_0)\,\mathrm{d}x_0$, one can rewrite (37) as

$$[\mathbf{S}]_{ji}^{nm}(a,b) = -\int_{-b}^{a} \tilde{N}_{ij}(x)\frac{\partial\phi_{mn}}{\partial x}(x,0,a,b)\,\mathrm{d}x.$$

After introducing the new variable λ, so that $x = x(\lambda) = \frac{1}{2}(a+b)\lambda + \frac{1}{2}(a-b)$, we obtain

$$[\mathbf{S}]_{ji}^{nm}(a,b) = -\frac{a+b}{2}\int_{-1}^{1} \tilde{N}_{ij}[x(\lambda)]\frac{\partial\phi_{mn}}{\partial x}\left[\frac{a+b}{2}\lambda + \frac{a-b}{2}, 0, a, b\right]\mathrm{d}\lambda. \tag{38}$$

The solution of problem (27)–(30) gives

$$\frac{\partial\phi_{mn}}{\partial x}\left(\frac{a+b}{2}\lambda + \frac{a-b}{2}, 0\right) = \frac{1}{\pi\sqrt{1-\lambda^2}} \times \mathbf{P}\cdot\mathbf{v}\cdot\int_{-1}^{1}\frac{\hat{N}_{mn}[x(\tau)]\sqrt{1-\tau^2}\,\mathrm{d}\tau}{\tau-\lambda}. \tag{39}$$

Substituting (39) into (38) and rearranging the result, it can be shown that all the elements of the added mass matrix can be analytically evaluated which makes the procedure very efficient. The same is true for the force vector $[\mathbf{f}_0]_{ji}$.

5. Dimensions of the contact region

In order to derive equations which govern motion of the contact points, we introduce the displacement potential $\psi(x,y,t)$ by equation

$$\psi(x,y,t) = \int_0^t \varphi(x,y,\tau)\,\mathrm{d}\tau. \tag{40}$$

The boundary-value problem for the new unknown function is obtained by integrating equations (15)–(18) with respect to time and taking into account initial conditions and the Wagner conditions (13) and (14). Then we obtain

$$\psi_{xx} + \psi_{yy} = 0 \quad (y < 0), \tag{41}$$

$$\psi = 0 \quad (x < -b, x > a, y = 0), \tag{42}$$

$$\psi_y = f(x) - t + w(x,t) \quad (-b < x < a), \tag{43}$$

$$\psi \to 0 \quad (x^2 + y^2 \to \infty). \tag{44}$$

Note that Eqs. (41)–(44) are similar to Eqs. (15)–(18), which are for the velocity potential. The main difference between these two systems of equations is due to the condition in the contact region. Now this condition is dependent on the shape of the entering body, see Eq. (43). The function $f(x)$ gives the distance between the initial position of the free surface and initial position of the entering body in vertical direction. Note that it does not matter which surface is curved. Only the initial distance between the impacting surfaces matters.

It is important to notice that the vertical derivative of the displacement potential provides the vertical displacement of liquid particles. Therefore, this derivative has to be bounded, in particular, at the contact points, $x = a(t)$ and $x = -b(t)$. The latter requirement provides two equations with respect to the unknown functions $a(t)$ and $b(t)$:

$$\lim_{x\to\pm 1}\int_{-1}^{1}\frac{G(\tau)\sqrt{1-\tau^2}\,\mathrm{d}\tau}{\tau - x} = 0, \tag{45}$$

$$G(\tau) = t - w[x(\tau), t] - f[x(\tau)], \tag{46}$$

$$x(\tau) = A\tau + B, \quad A = \frac{a+b}{2}, \quad B = \frac{a-b}{2}. \tag{47}$$

The quantity $A(t)$ is the radius of the contact region and $B(t)$ is a characteristic of the region asymmetry. In the symmetric case, $B = 0$.

There are two equations in (45), which can be written as

$$\int_{-1}^{1} G(\tau, A, B, t)\frac{\mathrm{d}\tau}{\sqrt{1-\tau^2}} = 0, \tag{48}$$

$$\int_{-1}^{1} \tau G(\tau, A, B, t)\frac{\mathrm{d}\tau}{\sqrt{1-\tau^2}} = 0. \tag{49}$$

It is convenient to take A as the new time-like variable and consider $t = t(A)$ and $B = B(A)$ as unknown functions of this variable. It is possible to reduce Eqs. (48) and (49) to ordinary differential equations with respect to the new unknown functions. These differential equations have to be added to system (34) and (35) and solved simultaneously.

We differentiate Eqs. (48) and (49) with respect to A and resolve the results with respect to derivatives $\mathrm{d}t/\mathrm{d}A$ and $\mathrm{d}B/\mathrm{d}A$. It is enough to perform the differentiation only for Eq. (48). Eq. (49) gives a similar result after introducing factor τ in the integrand. We obtain

$$\frac{\partial G}{\partial A}(\tau, A, B(A), t(A)) = \frac{\mathrm{d}t}{\mathrm{d}A} - \frac{\partial w}{\partial x}\left[\tau + \frac{\mathrm{d}B}{\mathrm{d}A}\right] - \frac{\mathrm{d}f}{\mathrm{d}x}\left[\tau + \frac{\mathrm{d}B}{\mathrm{d}A}\right] - \frac{\partial w}{\partial t}\frac{\mathrm{d}t}{\mathrm{d}A}, \tag{50}$$

which makes it possible to rewrite (48) after its differentiation in the form

$$a_{11}\frac{\mathrm{d}t}{\mathrm{d}A} - a_{12}\frac{\mathrm{d}B}{\mathrm{d}A} = f_1, \tag{51}$$

$$a_{11}(A, B, \mathbf{d}) = \int_{-1}^{1}\frac{1 - \dot{w}[x(\tau, A, B), t]}{\sqrt{1-\tau^2}}\,\mathrm{d}\tau, \tag{52}$$

$$a_{12}(A, B, \mathbf{a}) = \int_{-1}^{1}\frac{w_x[x(\tau), t] + f'[x(\tau)]}{\sqrt{1-\tau^2}}\,\mathrm{d}\tau, \tag{53}$$

$$f_1(A, B, \mathbf{a}) = \int_{-1}^{1}\frac{w_x[x(\tau), t] + f'[x(\tau)]}{\sqrt{1-\tau^2}}\tau\,\mathrm{d}\tau. \tag{54}$$

Correspondingly, Eq. (49) gives

$$a_{21}\frac{\mathrm{d}t}{\mathrm{d}A} - a_{22}\frac{\mathrm{d}B}{\mathrm{d}A} = f_2. \tag{55}$$

The coefficients a_{21}, a_{22} and f_2 are obtained following the same procedure. Substituting expansion (22) into (52), we find

$$a_{11}(A, B, \mathbf{d}) = \pi - \dot{\mathbf{a}}\mathbf{a}^{(11)}, \tag{56}$$

where $\dot{\mathbf{a}}$ is given by (35), the right-hand side of which is dependent on A, B and $\mathbf{d}$. Proceeding in a similar way, we obtain

$$a_{21}(A, B, \mathbf{d}) = -\dot{\mathbf{a}}\mathbf{a}^{(21)}, \tag{57}$$

the elements of the vectors $\mathbf{a}^{(11)}$ and $\mathbf{a}^{(21)}$ are dependent only on A and B and are calculated analytically.

Integrals (53) and (54) are evaluated in a similar way. Once the coefficients in equations (51) and (55) have been calculated, these equations can be presented as

$$\frac{\mathrm{d}t}{\mathrm{d}A} = Q_1(A, B, \mathbf{a}, \mathbf{d}), \quad \frac{\mathrm{d}B}{\mathrm{d}A} = Q_2(A, B, \mathbf{a}, \mathbf{d}). \tag{58}$$

Finally multiplying equations (34) and (35) by $\mathrm{d}t/\mathrm{d}A$, we obtain

$$\frac{\mathrm{d}\mathbf{d}}{\mathrm{d}A} = -\mathbf{Ka}\cdot Q_1, \tag{59}$$

$$\frac{\mathrm{d}\mathbf{a}}{\mathrm{d}A} = (\mathbf{M}+\mathbf{S}(a,b))^{-1}[\mathbf{d}-\mathbf{f}_0(a,b)]\,Q_1. \tag{60}$$

The system of ordinary differential equations (58)–(60) is solved numerically with the initial conditions $t=0$, $B=0$, $\mathbf{a}=0$, $\mathbf{d}=0$ at $A=0$.

6. Results and discussion

6.1. Added masses of elastic plate

As mentioned in the Introduction, the coupled problem (13)–(21) can be solved by the normal mode method in the case of a homogeneous beam. We consider the symmetric case, where the plate corresponds to the interval $-1<x<1$ in nondimensional variables and both the plate deflection $w(x,t)$ and the velocity potential are even with respect to the coordinate x. The plate is simply supported at its ends. In this case the beam deflection is sought in the form

$$w(x,t) = \sum_{n=1}^{\infty} a_n(t)\psi_n(x), \tag{61}$$

Table 1
Added mass coefficient S_{11} for $N=10$

a	S_{num}	S_{ana}	Relative error
0.1	0.0156110	0.0156113	2.2405E−05
0.2	0.0612987	0.0613005	2.8747E−05
0.3	0.1337342	0.1337377	2.6077E−05
0.4	0.2277072	0.2277134	2.7555E−05
0.5	0.3366057	0.3366147	2.6615E−05
0.6	0.4530144	0.4530267	2.7222E−05
0.7	0.5693887	0.5694039	2.6820E−05
0.8	0.6787272	0.6787456	2.7074E−05
0.9	0.7751922	0.7752130	2.6927E−05
1.0	0.8546074	0.8546305	2.7000E−05

Table 2
Added mass coefficient S_{11} for $N=20$

a	S_{num}	S_{ana}	Relative error
0.1	0.0156113	0.0156113	1.8038E−06
0.2	0.0613004	0.0613005	1.7318E−06
0.3	0.1337375	0.1337377	1.7109E−06
0.4	0.2277130	0.2277134	1.7002E−06
0.5	0.3366141	0.3366147	1.6936E−06
0.6	0.4530259	0.4530267	1.6895E−06
0.7	0.5694030	0.5694039	1.6875E−06
0.8	0.6787445	0.6787456	1.6874E−06
0.9	0.7752117	0.7752130	1.6885E−06
1.0	0.8546290	0.8546305	1.6904E−06

where $\psi_n(x) = \cos(\lambda_n x)$ and $\lambda_n = (n - 1/2)\pi$. Within the normal mode method the added mass matrix S_{mn} is defined as

$$S_{mn}(a) = \int_{-a}^{a} \phi_n(x, 0, a)\psi_m(x)\,\mathrm{d}x, \tag{62}$$

where $2a$ is the dimension of the wetted part of the beam and ϕ_n satisfies the boundary value problem similar to (27)–(30), the difference being in the boundary condition (29) for the wetted part which becomes:

$$\frac{\partial \phi_n}{\partial y} = \psi_n(x) \quad (y<0, |x|<a(t)). \tag{63}$$

After some algebra (see Korobkin, 1998), we obtain for $S_{mn}(a)$

$$S_{mn}(a) = \frac{\pi a}{\lambda_n^2 - \lambda_m^2}[\lambda_n J_0(\lambda_m a)J_1(\lambda_n a) - \lambda_m J_0(\lambda_n a)J_1(\lambda_m a)] \quad (n \neq m), \tag{64}$$

$$S_{nn}(a) = \frac{\pi}{2}a^2[J_0^2(\lambda_n a) + J_1^2(\lambda_n a)]. \tag{65}$$

The elements of the matrix S can be also computed with the help of the finite element method. Defining the coefficients f_{ij}^n so that

$$\psi_n(x) = \cos(\lambda_n x) \approx \sum_{j=1}^{N}\sum_{i=1}^{4} f_{ij}^n N_{ij}(\xi) \tag{66}$$

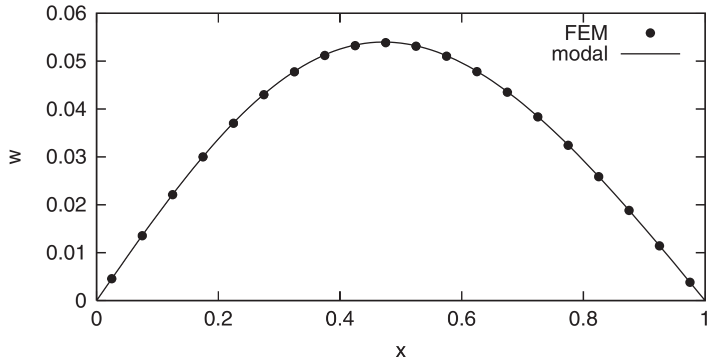

Fig. 2. Plate deflection.

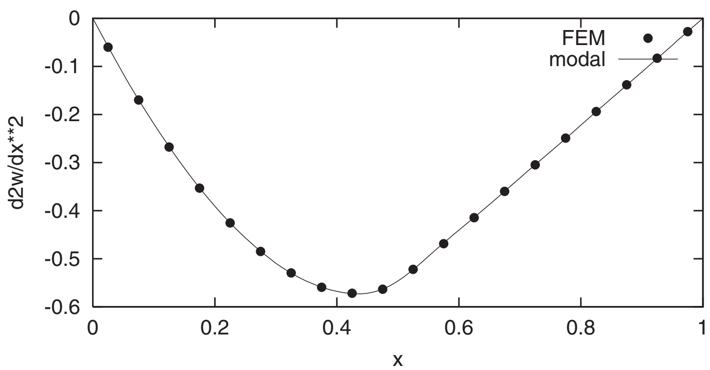

Fig. 3. Second derivative obtained by modal and FEM approach.

one can find

$$S_{\alpha,\beta} \approx \sum_{n=1}^{N}\sum_{m=1}^{4} f_{nm}^{\alpha} \sum_{j=1}^{N}\sum_{i=1}^{4} f_{nm}^{\beta}[S]_{ji}^{nm}, \tag{67}$$

where $[S]_{ji}^{nm}$ were defined in Section 4.

In Tables 1 and 2 we show the comparison between the analytical results (65) for S_{11} and those obtained using the finite element representation (67) for two numbers of finite elements, $N = 10$ and $N = 20$. We can observe very good convergence characteristics of the finite element method.

6.2. Numerical slamming simulation

In Figs. 2 and 3 we show the results for the nondimensional deflection, and its second derivative, of the wedge right plating during impact, obtained by the present method and the normal mode method [see Korobkin (2000)]. The plate is simply supported at its edges, the half-length L equals 0.5 m, the beam thickness is 1 cm, its density 7850 kg/m^3, deadrise angle γ is 10° degrees, and the impact velocity equals 4 m/s. The time corresponds to the instant where the plate is half wetted. We can see very good agreement between the two methods.

It should be noted that the normal mode method is not well suited to numerical analysis of elastic wedge impact. This is due to the fact that the wedge consists of two independent beams, which interact only if both beams are in contact with water. The problem is tackled by the normal mode method in Korobkin (2000) only in the symmetric case, when the beams behave identically. We do not know at present how to solve the asymmetric problem of elastic wedge impact by the normal mode method. However, even in the symmetric case, the application of the normal mode method to the elastic wedge impact problem is non-trivial and requires many modes to achieve convergence of the numerical solution. If for one homogeneous beam the normal mode method requires about 10 modes to provide accurate results [see Korobkin (1998)], the elastic wedge case requires more than 100 modes to provide a reasonable result. The lines in Figs. 2 and 3 are obtained with 150 modes. The corresponding CPU time of the normal mode method is too large; this is why this method cannot be recommended for practical problems of complicated structural impact on the water surface.

7. Conclusion

A method for the calculation of hydroelastic impact has been developed on the basis of Wagner theory for fluid flow and a finite element representation of the structure. All intermediate steps of the analysis are carefully checked and the method is validated by comparisons with the modal method using a beam model for the structure.

Further developments concern the coupling of the method with more realistic models for the impacting structure by using general finite element codes. Two strategies are possible: *direct coupling* and *modal approach*.

In the direct coupling approach, we follow the method described in the present paper, except that the interaction is restricted to the wetted part of the finite element model. The disadvantage of the method may be the relatively big system of dynamic equations (for each node of the whole structural model) which have to be integrated in time. The system is no longer diagonally dominant due to the added mass associated with the wetted nodes. Also, the transfer of information between the two models may not be straightforward.

In the modal approach, the structural modes (dry) are first calculated, and the modal characteristics (mass, stiffness and displacements of the interface) are transferred to the hydrodynamic solver which calculates the associated hydrodynamic coefficients using the finite element generic solutions explained in Section 6.1. The dynamic equations for the principal coordinates of the modes are than integrated in time and modal amplitude time histories are retransferred to the FEM code in order to generate the time history of the displacements and strains in the whole structure. The advantage of this method is that the coupling procedure is quite clear and the system of equations to integrate in time is of lower order (equal to the number of retained modes). The weakness may lie in the representation of very high impact loads where the number of necessary modes increases, especially in the first few time instants. In this respect, the choice of the method will depend on the nature of the impact and on the type of information required.

References

Arai, M., Miyauchi, T., 1998. Numerical study of the impact of water on cylindrical shells considering fluid–structure interactions. In: Proceedings of 6th International Symposium on Practical Design of Ships and Mobile Units (PRADS). The Hague, The Netherlands, pp. 59–68.

Cointe, R., 1991. Free-surface flows close to a surface-piercing body. In: Miloh, T. (Ed.), Mathematical Approaches in Hydrodynamics. SIAM, Philadelphia, PA, pp. 319–334.

Faltinsen, O.M., 1997. The effect of hydroelasticity on ship slamming. Philosophical Transactions of the Royal Society of London, Series A, Mathematical and Physical Sciences 355, 575–591.

Faltinsen, O.M., Kvalsvold, J., Aarsnes, J.V., 1997. Wave impact on a horizontal elastic plate. Journal of Marine Science and Technology 2, 87–100.

Fraenkel, L.E., McLeod, J.B., 1997. Some results for the entry of a blunt wedge into water. Philosophical Transactions of the Royal Society of London, Series A, Mathematical and Physical Sciences 355, 523–535.

Howison, S.D., Ockendon, J.R., Wilson, S.K., 1991. Incompressible water-entry problems at small deadrise angles. Journal of Fluid Mechanics 222, 215–230.

Ionina, M., Korobkin, A.A., 1999. Water impact on cylindrical shells. In: Proceedings of 14th Workshop on Water Waves and Floating Bodies. Michigan, USA, pp. 44–47.

Korobkin, A.A., 1998. Wave impact on the center of an Euler beam. Journal of Applied Mechanics and Technical Physics 39, 770–781.

Korobkin, A.A., 2000. Elastic Wedge Impact. Lecture 1, Lecture Notes, INSEAN.

Korobkin, A.A., 2004. Analytical models of water impact. European Journal of Applied Mathematics 15, 821–838.

Kvalsvold, J., Faltinsen, O.M., 1995. Hydroelastic modelling of wetdeck slamming on multihull vessels. Journal of Ship Research 39, 225–239.

Lu, C.H., He, Y.S., Wu, G.X., 2000. Coupled analysis of nonlinear interaction between fluid and structure during impact. Journal of Fluids and Structures 14, 127–146.

Malenica, Š., 1998. Hydroelastic coupling of beam structural model with 3D hydrodynamic model. In: Proceedings of the Second International Conference on Hydroelasticity in Marine Technology. Kyushu, Japan, pp. 507–512.

Mei, X., Liu, Y., Yue, D.K.P., 1999. On the water impact of general two-dimensional sections. Applied Ocean Research 21, 1–15.

Oliver, J.M., 2002. Water entry and related problems. Ph.D. Thesis, University of Oxford, UK.

Wagner, H., 1932. Über Stoss- und Gleitvergänge an der Oberfläche von Flüssigkeiten. Zeitschrift für angewandte Mathematik und Mechanik 12, 193–215.

Zhao, R., Faltinsen, O.M., Aarsnes, J.V., 1996. Water entry of arbitrary two-dimensional sections with and without separation. In: Proceedings of 21st Symposium on Naval Hydrodynamics. Trondheim, Norway, pp. 118–133.